

# RSC Advances



This is an *Accepted Manuscript*, which has been through the Royal Society of Chemistry peer review process and has been accepted for publication.

*Accepted Manuscripts* are published online shortly after acceptance, before technical editing, formatting and proof reading. Using this free service, authors can make their results available to the community, in citable form, before we publish the edited article. This *Accepted Manuscript* will be replaced by the edited, formatted and paginated article as soon as this is available.

You can find more information about *Accepted Manuscripts* in the [Information for Authors](#).

Please note that technical editing may introduce minor changes to the text and/or graphics, which may alter content. The journal's standard [Terms & Conditions](#) and the [Ethical guidelines](#) still apply. In no event shall the Royal Society of Chemistry be held responsible for any errors or omissions in this *Accepted Manuscript* or any consequences arising from the use of any information it contains.

# A Simple and Reversible Fluorescent Probe Based on NBD for Rapid Detection of Hypochlorite and Its Application for Bioimaging

Youming Shen,<sup>ab</sup> Xiangyang Zhang,<sup>\*a</sup> Xi Huang,<sup>b</sup> Siyu Wen,<sup>a</sup> Mingdi Liu,<sup>a</sup> Yan Deng,<sup>a</sup> Youyu Zhang,<sup>\*b</sup> Chunxiang Zhang,<sup>a</sup> Junling Jin,<sup>a</sup> Haitao Li,<sup>b</sup> and Shouzhuo Yao<sup>b</sup>

<sup>a</sup> College of Chemistry and Chemical Engineering, Hunan University of Arts and Science, ChangDe, 415000, PR China E-mail: zhangxiangy06@163.com

<sup>b</sup> Key Laboratory of Chemical Biology and Traditional Chinese Medicine Research (Ministry of Education), College of Chemistry and Chemical Engineering, Hunan Normal University, Changsha 410081, PR China E-mail: zhangyy@hunnu.edu.cn

## Abstract

A simple and reversible fluorescent probe bearing 7-nitrobenz-2-oxa-1,3-diazole and selenomorpholine fragment was designed and synthesized. The probe showed highly selective, sensitive and fast (<10 s) recognition to hypochlorite in aqueous solutions. The relative results demonstrated that the linear response range of the probe was between  $5.0 \times 10^{-8}$  M and  $1.2 \times 10^{-4}$  M, with a low detection limit of 3.3 nM ( $S/N = 3$ ). The probe was capable of monitoring hypochlorite reversibly in the presence of glutathione. In addition, the biological applications in living cells have been described.

**Keywords:** Hypochlorite; Fluorescent probe; 7-nitrobenz-2-oxa-1,3-diazole; Selenide

## 1 Introduction

Hypochlorite ( $\text{ClO}^-$ ) is one of the most significant reactive oxygen species (ROS) in biological systems and plays a critical role in many biological processes. [1] It is produced from the reaction of  $\text{H}_2\text{O}_2$  with chloride ions catalyzed by a heme enzyme myeloperoxidase (MPO) in living systems. [2] However, a high concentration of hypochlorite can cause tissue damage and a variety of pathological diseases including neuron degeneration, [3] inflammatory disease, [4] atherosclerosis, [5] cystic fibrosis, [6] arthritis, [7] cardiovascular disease, [8] cancers, [9] and liver cirrhosis. [10] When oxidative damage occurs in living cells, the antioxidative and repair mechanisms of living organisms start to protect essential components of cells against the hypochlorite harm at once. [11] Therefore, it is worth developing a highly sensitive, good selective and fast technique to monitor the redox changes between hypochlorite and antioxidants in living organisms.

Fluorescence sensing are efficient ways for detecting species both in solution and living organism due to their excellent selectivity, high sensitivity, ability for real-time capability and fast response times. So far, fluorescence sensors for specific detection of hypochlorite have been constructed based on the strong oxidation properties of hypochlorite. These probes were generally designed on the basis of the conjugation of a fluorophore with a hypochlorite reactive group, such as p-methoxyphenol, p-alkoxyaniline, dibenzoylhydrazine, hydroxamic acid, thiol, and oxim derivatives. [12] These oxidation-reaction based probes were very useful for sensing for hypochlorite, however, most of them have not realized to detect hypochlorite based on

the redox cycle. The complex redox biology of the cell governs many essential biological processes and has broad implications in human health and diseases. [13] Thus, it is eagerly desirable to design and develop reversible fluorescent probes.

Selenium (Se) is a compound with various oxidations and it is applicable to the design of reversible ROS probes *via* the oxidation-reduction cycles. [14] In the past few years, Se containing fluorophores have been used for designing reversible fluorescent probes for detecting hypochlorite. [15] For example, Liu et al reported a BODIPY-based fluorescent probe which can reversibly recognize hypochlorite. [15b] Lou et al developed a reversible fluorescent probe for hypochlorite acid based on 1,8-naphthalimide. [15g] The probes could respond reversibly for the redox changes mediated by hypochlorite acid and thiols. The reversibly fluorescent probes are suitable for visualizing states of redox stress and continuous monitoring of real-time hypochlorite. However, some of them still encounter some problems, such as low sensitivity, complicated synthetic procedures and long response time. These limitations seriously retarded the application of the probe in real biological. In this regard, it is worth designing and developing new reversible fluorescent probes being able to overcome these limitations in detecting hypochlorite.

The present study about fluorescent probes for detection of hypochlorite was mainly focused on the selection of dyes and recognition fragment. Heptamethine cyanine dye, 1, 8-naphthalimide dye, BODIPY dye and other dyes have been widely utilized to explore chemosensors for hypochlorite. [16,17] However, to the best of our knowledge, there are few studies and applications of visual and

fluorometric sensor based on NBD for highly sensitive and reversible detection of hypochlorite up to now.

7-Nitrobenz-2-oxa-1,3-diazole (NBD) derivatives have been extensively used in fluorescent labeling reagents because of their good spectral properties, excellent biocompatibility, cellular membrane-penetrating capacity, commercial availability and easy functionalization. [18] Currently, based on the photoinduced electron transfer (PET) mechanism, NBD derivatives have been used as fluorescent chemosensors for detecting heavy metal ions. [19] According to the PET mechanism, we begin to consider a fluorometric sensing integrated with NBD as signaling unit and selenomorpholin as a recognition group for detection of hypochlorite. We envisage when NBD is conjugated with selenide, the fluorescence of the probe is weak. NBD-selenide is oxidized to selenoxide by hypochlorite, the fluorescence of NBD-selenide will increase because of the electron-withdrawing effect of NBD-selenoxide. Once NBD-selenoxide is reduced to NBD-selenide by antioxidants, the fluorescence of NBD-selenide recovers its original weak fluorescence again. In this way, the NBD-selenide is expected to acquire positive results for reversible detection of hypochlorite.

With these considerations in mind, we decided to incorporate the selenomorpholin moiety into the NBD core *via* a simple substitution reaction, obtaining a novel and reversible probe for visualizing the redox changes mediated by hypochlorite and glutathione (GSH). As shown in Figure 1, compound **1** contains a NBD dye and selenomorpholin moiety for hypochlorite.

As expected, compound **1** itself is weak fluorescent, whereas it showed fluorescence intensity change response between hypochlorite and GSH in aqueous media. Moreover, compound **1** can serve as a naked-eye indicator for hypochlorite by color change. In addition, compound **1** could be successfully applied for hypochlorite detection in living cells. Notably, this novel and simple NBD-selenide based visual and turn on fluorescent probe for highly selective, sensitive and fast (<10 s) detection of hypochlorite with a low detection limit (3.3 nM) will fit the preference of further application.

## 2 Experimental

### 2.1 Reagents and chemicals

4-chloro-7-nitro-benzoxadiazole (NBD-Cl) was purchased from Sigma-Aldrich Company. All other chemicals used in this work were of analytical grade, purchased from Sinopharm chemical reagent company and used without further purification. The synthesis of selenomorpholine was similar to the procedures reported by Hu Liming et al. [20] The thin-layer chromatography (TLC) was carried out on silica gel plates (60F-254) using UV-light to monitor the reaction, and Silica gel (200-300 mesh) was used for column chromatography. Milli-Q ultrapure water (Millipore,  $\geq 18$  M cm) was used throughout. Various ROS and RNS including  $\bullet\text{OH}$ ,  $\text{NO}_3^-$ ,  $\text{NO}_2^-$ ,  $\text{ONOO}^-$ ,  $^1\text{O}_2$ ,  $\text{O}_2^{2-}$ , NO and t-BuOOH were prepared according to published methods. [21]

### 2.2 Instrumentation

Fluorescence spectra were carried out using a Hitachi F-7000 spectrophotometer. UV-Vis spectra were measured on a Shimadzu UV2450 spectrophotometer.

Fluorescence imaging of Hela cells was carried out using fluorescence microscopy.  $^1\text{H}$  NMR and  $^{13}\text{C}$  NMR spectra were recorded using a Bruker AVB-500 MHz NMR spectrometer (Bruker biospin, Switzerland). Mass spectra were obtained using a Bruker Daltonics BioTOF-Q mass spectrometer in the positive mode. The pH measurements were performed with a Sartorius basic pH-meter PB-10.

### 2.3 Synthesis of compound 1

*(Preferred position for scheme 1)*

As illustrated in Scheme 1, compound 1 was readily prepared in one step method. Briefly, to a solution of 4-chloro-7-nitro-benzoxadiazole (NBD-Cl) (0.2 g, 1 mmol) in 5 mL  $\text{CH}_2\text{Cl}_2$ , selenomorpholinol (0.15 g, 1 mmol) and  $\text{Et}_3\text{N}$  (0.12 g, 1.2 mmol) were added. The mixture was stirred at room temperature for 4 h under  $\text{N}_2$  atmosphere. Then, a rude mixture was concentrated under reduced pressure. The residue was purified by silica gel column chromatography (petroleum ether / ethyl acetate, 4:1,  $V/V$ ) to give compound 1 in 85% yield (0.27 g).  $^1\text{H}$  NMR ( $\text{CDCl}_3$ , 500 MHz)  $\delta$ (ppm): 8.46 (d,  $J = 9.0$  Hz, 1H), 6.28 (d,  $J = 9.0$  Hz, 1H), 4.57 (t,  $J = 5.0$  Hz, 4H), 2.93 (t,  $J = 5.0$  Hz, 4H);  $^{13}\text{C}$  NMR ( $\text{CDCl}_3$ , 125 MHz)  $\delta$ (ppm): 145.0, 144.8, 145.8, 144.0, 135.1, 123.6, 102.6, 53.3, 16.8; ESI-MS  $m/z$   $[\text{M}+\text{Na}]^+$  calc 336.1612, obs 336.9810.

### 2.4 Measurement procedure

A stock solution of compound 1 was prepared by dissolving compound 1 in acetonitrile. Fluorescence and absorption spectra were recorded in acetonitrile-water solution (1:1 v/v, 50 mM PBS buffer solution at pH 7.4). The fluorescence intensity was recorded with a fluorescence spectrometer ( $\lambda_{\text{ex}} = 468$  nm,  $\lambda_{\text{em}} = 544$  nm, slit: 10

nm / 10 nm).

## 2.5 Cell culture

The HeLa cells were incubated on a 96-well plate and allowed to adhere for 24 h at 37°C, and then washed three times with PBS and incubated at 37°C in the presence of compound **1** (10 μM, 1 : 99 DMSO-PBS, v/v, pH 7.4) for 30 minute. Then the cells were washed three times with PBS buffer and incubated at 37°C in the presence of NaClO for 10 minute. The fluorescence images were recorded using an inverted fluorescence microscope (NIKON Eclipse Ti-S, Japan) with a 20 x objective lens.

## 2.6 Determination of fluorescence quantum yield

The fluorescence quantum yield was determined using the solutions of fluorescein ( $\Phi_F = 0.90$  in 0.1N NaOH [22]) as reference. The quantum yield was calculated using the following equation:

$$\Phi_{F(s)} = \Phi_{F(r)} (F_s A_r / F_r A_s) (n_s / n_r)^2$$

Where  $\Phi_F$  is the fluorescence quantum yield, F is the area under the corrected emission curve, A is the absorbance at the excitation wavelength and n is the refractive index of the solvents used. Subscripts refer to the reference (r) or sample (s) compound.

## 3 Results and discussion

### 3.1 Spectra properties of compound **1**

*(Preferred position for Fig. 1)*

The fluorescence properties of the compound **1** were studied in CH<sub>3</sub>CN-H<sub>2</sub>O solution (1:1 v/v, 50 mM PBS buffer solution at pH 7.4). The compound **1** itself

displays weak fluorescence ( $\Phi = 0.002$ ), which suggested the PET process from Se atom to NBD fluorophore occurred. Upon addition of  $\text{ClO}^-$ , the fluorescence intensity of the compound **1** at 544 nm increases steadily (Fig. 1a). After 120  $\mu\text{M}$  of  $\text{ClO}^-$  was added, the fluorescence intensity enhanced up to 32-fold, and the final quantum yield was 0.048. The results implied that the PET process in compound **1** was inhibited upon the addition of  $\text{ClO}^-$ , in good agreement with our design. Moreover, the fluorescence intensity of compound **1** at 544 nm showed a good linear response to  $\text{ClO}^-$  in the range of  $5 \times 10^{-8}$  M to  $1.20 \times 10^{-4}$  M (Fig. 1B). The detection limit for  $\text{ClO}^-$  is estimated to be 3.3 nM ( $S / N = 3$ ). The low detection limit shown that compound **1** is highly sensitive to  $\text{ClO}^-$ .

To further get insight into the reaction of  $\text{ClO}^-$  with compound **1**, the UV spectrum of compound **1** in the absence and in the presence of  $\text{ClO}^-$  were investigated. As depicted in Fig. 2, compound **1** itself displayed absorption centered at 344 nm and 483 nm. However, upon addition of 12 eqv. of  $\text{ClO}^-$  to a solution of compound **1**, the absorbance bands of compound **1** were recorded with a blue-shift to 294 nm and 468 nm respectively. Blue-shift in absorption spectra further demonstrated that compound **1** can react with  $\text{ClO}^-$ . Concurrently, an obvious color change from orange to yellow was observed (Fig. 2, inset). This phenomenon indicates that compound **1** can be employed conveniently for  $\text{ClO}^-$  detection by simple visual inspection.

*(Preferred position for Fig. 2)*

### 3.2 Effects of reaction time on sensing $\text{ClO}^-$

Reaction time is an important factor for reaction-based probes, and the

time-dependent fluorescence spectra of compound **1** in the presence of  $\text{ClO}^-$  were examined. As shown in Fig. 3, the fluorescence intensity of compound **1** at 544 nm shows no obvious variations in the absence of  $\text{ClO}^-$ , which proves that compound **1** is very stable in such a sensing system. When 50  $\mu\text{M}$  and 120  $\mu\text{M}$  of  $\text{ClO}^-$  was added respectively, the fluorescence intensities enhanced within just a few seconds ( $<10$  s) at 544 nm, and the fluorescence intensity remained nearly unchanged over time. Therefore, compound **1** is a good candidate for real-time detection of  $\text{ClO}^-$ .

*(Preferred position for Fig. 3)*

### 3.3 Influence of pH value

To test the application extent of compound **1** as a  $\text{ClO}^-$  probe, the fluorescence properties of the compound **1** was investigated both in the absence and presence of  $\text{ClO}^-$  in different pH values ranging from 1 to 12.0 (Fig. 4). As can be seen in Fig. 4, in the absence of  $\text{ClO}^-$ , compound **1** did not exhibit any fluorescence changes in the pH range of 1.0 - 12.0, and showed weak fluorescence at 544 nm. However, the solution pH is between 4.0 and 12.0, a fluorescence increase was induced in the presence of 12 eqv.  $\text{ClO}^-$ . When the pH value was between 7.0 and 8.0, the the strong fluorescence was detectable at 544 nm. This indicated that compound **1** is pH-dependence in the detection of  $\text{ClO}^-$ , and it could be used to detect  $\text{ClO}^-$  at physiological conditions.

*(Preferred position for Fig. 4)*

### 3.4 Selectivity of compound **1**

To evaluate the compound **1** as a highly selective chemosensor for  $\text{ClO}^-$  under simulated physiological conditions (pH = 7.4), we investigated the responses of compound **1** to various analytes including a series of ROS / RNS ( $\cdot\text{OH}$ ,  $\text{ONOO}^-$ ,  $^1\text{O}_2$ ,  $\text{O}_2^-$ ,  $\text{NO}$ ,  $\text{H}_2\text{O}_2$ ,  $t\text{-BuOOH}$ ,  $\text{NO}_2^-$ ,  $\text{ClO}^-$  and  $\text{NO}_3^-$ ) and metal ions ( $\text{Fe}^{3+}$ ,  $\text{Cu}^{2+}$  and  $\text{Hg}^{2+}$ ). As displayed in Fig. 5, the fluorescence of compound **1** at 544 nm was a dramatic increase with  $\text{ClO}^-$ , no obvious fluorescence enhancement was observed for any analyte. The excellent selectivity toward  $\text{ClO}^-$  over other interfering species exhibits that compound **1** has the potential to detect  $\text{ClO}^-$  in biological environment.

*(Preferred position for Fig. 5)*

### 3.5 Reversibility of compound **1**

To examine reversibility of compound **1**, the fluorescence intensity of compound **1** were mediated by  $\text{ClO}^-$  and GSH in  $\text{CH}_3\text{CN-H}_2\text{O}$  solution (1:1 v/v, 50 mM PBS buffer solution at pH 7.4). As shown in Fig. 6, when upon addition of  $\text{ClO}^-$  to a solution of compound **1**, fluorescence intensity reached a maximum value. Then GSH was added to the above solution, the fluorescence intensity showed decrease and recovered its weak fluorescence. This reversible redox cycle can be repeated at least four times under the same conditions. These results showed that compound **1** could be used to detect  $\text{ClO}^-$  continuously.

*(Preferred position for Fig. 6)*

### 3.6 Investigation of sensing mechanism

*(Preferred position for scheme 2)*

In our hypothesis, compound **1** exhibited faint fluorescence due to the PET process from the selenide to NBD in the excited state. After the reaction with  $\text{ClO}^-$ , the fluorescence of compound **1** would boost because of the resulting the hampered PET process induced by the formation of selenoxide. Once reduction of selenoxide to selenide was triggered by GSH, the fluorescence switch was turned off, and the compound **1** recovered its weak fluorescence. To verify the proposed mechanism, a Job plot of compound **1** reaction with  $\text{ClO}^-$  was examined, and the result displayed compound **1** reacted  $\text{ClO}^-$  in a 1:1 molar ration (Fig.7). The mass spectrum of the reaction of compound **1** with NaClO showed one new peaks with  $m/z$  of 330.9940, which can be assigned as  $[\mathbf{1-O}+1]^+$ . This result indicated that compound **1** with  $m/z$  of 336.9814 for  $[\mathbf{1}+\text{Na}]^+$  can be converted into **1-O** in the presence of NaClO (Fig.S5 in the supporting information). Thus, the experiment results confirmed the proposed reaction mechanism, a possible mechanism was proposed as shown in Scheme 2.

*(Preferred position for Fig. 7)*

### 3.7 Biological imaging studies

In order to further explore the potential biological application of this sensor, the real-time imaging of cellular redox cycles was evaluated in Hela cells (Fig. 8). The Hela cells was incubated with compound **1** (10  $\mu\text{M}$ ) for 30 minute at  $37^\circ\text{C}$ , and a dark fluorescence was recorded. Then a strong fluorescence was appeared after the addition of 30  $\mu\text{M}$  NaClO into the medium and incubation for another 10 minute at  $37^\circ\text{C}$ , which indicating a good cell-membrane permeability of compound **1**. When stimulating compound **1**-loaded cells with 100  $\mu\text{M}$  GSH for 10 minute after removal

of the remaining NaClO, no fluorescence was observed. This indicates that the NBD-selenoxide was reduced to the nonfluorescent NBD-selenide by GSH. Those experiment results suggested that compound **1** had a good reversibility and could monitor the redox status in cells.

*(Preferred position for scheme Fig.8)*

*(Preferred position for Table 1)*

#### **4 Conclusion**

In summary, we have developed a simple and novel probe for ClO<sup>-</sup> by combining NBD moiety as the fluorophore and selenide as the recognition unit. Compared with some reported fluorescent probes for hypochlorite determination (Table 1), the proposed fluorescent probe for ClO<sup>-</sup> displayed several advantages in terms of high selectivity, reversibility, speedy response and a low detection limit. In addition, fluorescent imaging of intracellular showed that compound **1** could be used to evaluate ClO<sup>-</sup> in biological systems. This strategy may provide a simple method to fabricate a chemical sensor in relevant biological processes of redox biology.

#### **Acknowledgments**

This work was supported by the National Natural Science Foundation of China (21342012, 21375037, 21507028), Hunan Provincial Natural Science Foundation of China (11JJ3023, 15JJ3094), Science and Technology Department (13JJ2020), State Key Laboratory of Chemo/Biosensing and Chemometrics Foundation (KLCBTC MR 2011-05), and Scientific Research Fund of Hunan Provincial Education Department (13C635).

## References

- 1 C. C. Winterbourn, M. B. Hampton, J. H. Livesey, A. J. Kettle, *J. Biol. Chem.*, 2006, **281**, 39860-39869.
- 2 (a) J. E. Harrison, J. Schultz, *J. Biol. Chem.*, 1976, **251**, 1371-1374; (b) Z. M. Prokopowicz, F. Arce, R. Biedron, C. L. Chiang, M. Ciszek, D. R. Katz, M. Nowakowska, S. Zapotoczny, J. Marcinkiewicz, B. M. Chain, *J. Immunol.*, 2010, **184**, 824-835.
- 3 D. I. Pattison, M. J. Davies, *Chem. Res. Toxicol.*, 2001, **14**, 1453-1464.
- 4 S. Sugiyama, K. Kugiyama, M. Aikawa, S. Nakamura, H. Ogawa, P. Libby, *Arterioscler., Thromb., Vasc. Biol.* 2004, **24**, 1309-1314.
- 5 A. Daugherty, J. L. Dunn, D. L. Rateri, J. W. Heinecke, *J. Clin. Invest.*, 1994, **94**, 437-444.
- 6 V. Rudolph, R. P. Andrie, T. K. Rudolph, K. Friedrichs, A. Klinke, B. Hirsch-Hoffmann, A. P. Schwoerer, D. Lau, X. M. Fu, K. Klingel, K. Sydow, M. Didie, A. Seniuk, E. C. von Leitner, K. Szoecs, J. W. Schrickel, H. Treede, U. Wenzel, T. Lewalter, G. Nickenig, W. H. Zimmermann, T. Meinertz, R. H. Boger, H. Reichen-spurner, B. A. Freeman, T. Eschenhagen, H. Ehmke, S. L. Hazen, S. Willems, S. Baldus, *Nat. Med.*, 2010, **16**, 470-474.
- 7 M. J. Steinbeck, L. J. Nesti, P. F. Sharkey, J. Parvizi, *J. Orthop. Res.*, 2007, **25**, 1128-1135.
- 8 W. Y. Lin, L. L. Long, *Chem. Eur. J.*, 2009, **15**, 2305-2309.
- 9 M. Benhar, D. Engelberg, A. Levitzki, *EMBO Rep.*, 2002, **3**, 420-425.

- 10 M. Whiteman, P. Rose, J. L. Siau, N. S. Cheung, G. S. Tan, B. Halliwell, J. S. Arm-strong. *Free Radic. Biol. Med.*, 2005, **38**, 1571-1584.
- 11 (a) A. Maritim, R. Sanders and J. Watkins III, *J. Biochem. Mol. Toxicol.*, 2003, **17**, 24-38; (b) I. Juránek, S. Bezek, *Gen. Physiol. Biophys.*, 2005, **24**, 263-278.
- 12 (a) Z. R Lou, P. Li, P. Song, K. L Han. *Analyst*, 2013, **138**, 6291-6295; (b) J. J. Hu, N. K. Wong, Q. Gu, X. Bai, S. Ye, D. Yang, *Org. Lett.*, 2014, **16**, 3544-3547; (c) L. Yuan, W. Lin, J. Song, Y. Yang, *Chem. Commun.*, 2011, **47**, 12691-12693; (d) S. Yu, C. Hsu, W. Chen, L. Wei, S. Wu, *Sens. Actuators B*, 2014, **196**, 203-207; (e) Y. Koide, Y. Urano, K. Hanaoka, T. Terai, T. Nagano, *J. Am. Chem. Soc.*, 2011, **133**, 5680-5682; (f) S. R. Liu, S. P. Wu, *Org. Lett.*, 2013, **15**, 878-881; (g) S. R. Liu, M. Vedamalai, S. P. Wu, *Anal. Chim. Acta*, 2013, **800**, 71-76; (h) Q. Xu, K. A. Lee, S. Lee, K. M. Lee, W. J. Lee, J. Yoon, *J. Am. Chem. Soc.*, 2013, **135**, 9944-9949; (i) M. Emrullahoglu, M. Ucuncu, E. Karakus, *Chem. Commun.*, 2013, **49**, 7836-7838; (j) G. Cheng, J. Fan, W. Sun, J. Cao, C. Hu, X. Peng, *Chem. Commun.*, 2014, **50**, 1018-1020; (k) X. Cheng, H. Jia, T. Long, J. Feng, J. Qin, Z. Li, *Chem. Commun.*, 2011, **47**, 11978-11980; (l) J. Kim, Y. Kim, *Analyst*, 2014, **139**, 2986-2989; (m) J. Li, F. Huo, C. Yin, *RSC Adv.*, 2014, **4**, 44610-44613; (n) Y. Zhou, J. Y. Li, K. H. Chu, K. Liu, C. Yao, J. Y. Li, *Chem. Commun.*, 2012, **48**, 4677-4679; (o) F. Liu, Y. Gao, J. Wang, S. Sun, *Analyst*, 2014, **139**, 3324-3329; (p) G. Li, D. Zhu, Q. Liu, L. Xue, H. Jiang, *Org. Lett.*, 2013, **15**, 2002-2005.
- 13 (a) Y. Koide, M. Kawaguchi, Y. Urano, K. Hanaoka, T. Komatsu, M. Abo, T. Teraia, T. Nagano, *Chem. Commun.*, 2012, **48**, 3091-3093; (b) B. C. Dickinson, J. Peltier, D.

- Stone, D. V. Schaffer, C. J. Chang, *Nat. Chem. Biol.*, 2011, **7**, 106-112; (c) E. W. Miller, S. X. Bian, C. J. Chang, *J. Am. Chem. Soc.*, 2007, **129**, 3458-3459.
- 14 J. T. Rotruck, A. L. Pope, H. E. Ganther, A. B. Swanson, D. G. Hafeman, W. G. Hoekstra, *Science*, 1973, **179**, 588-590.
- 15 (a) B. Wang, P. Li, F. Yu, J. Chen, Z. Qu, K. Han, *Chem. Commun.*, 2013, 49, 5790-5792; (b) S. R. Liu, S. P. Wu, *Org. Lett.*, 2013, **15**, 878-881; (c) B. S. Wang, P. Li, F.B. Yu, P. Song, X. F. Sun, S. Q. Yang, Z. R. Lou, K. L. Han. *Chem. Commun.*, 2013, **49**, 1014-1016; (d) Z. R. Lou, P. Li, Q. Pan, K. L. Han. *Chem. Commun.*, 2013, **49**, 2445--2447.
- 16 X. Q. Chen, X. Z. Tian, I. Shin, J. Y. Yoon, *Chem. Soc. Rev.*, 2011, **40**, 4783-4804.
- 17 S. T. Manjare, J. Kim, Y. Lee, D. G. Churchill, *Org. Lett.*, 2014, **16**, 520-523.
- 18 L. D. Lavis, R.T. Raines, *ACS Chem. Biol.*, 2008, **3**, 142-155.
- 19 (a) W. Jiang, Q. Fu, H. Fan and W. Wang, *Chem. Commun.*, 2008, **14**, 259-261; (b) F. Qian, C. Zhang, Y. Zhang, W. He, X. Gao, P. Hu and Z. Guo, *J. Am. Chem. Soc.*, 2009, **131**, 1460-1468; (c) S. Banthia and A. Samanta, *New Journal of Chemistry*, 2005, **29**, 1007-1010; (d) S. H. Kim, J. S. Kim, S. M. Park and S. K. Chang, *Organic Letters*, 2006, **8**, 371-374; (e) Y. M. Shen, Y. Y. Zhang, X. Y. Zhang, C. X. Zhang, L. Zhang, J. L. Jin, H. T. Li and S. Z. Yao, *Anal. Methods*, 2014, **6**, 4797-4802; (f) Z. Xie, K. Wang, C. Zhang, Z. Yang, Y. Chen, Z. Guo, G.-Y. Lu and W. He, *New Journal of Chemistry*, 2011, **35**, 607-613; (g) H. J. Jeong, Y. Li and M. H. Hyun, *Bulletin of the Korean Chemical Society*, 2011, **32**, 2809-2812; (h) Y. B. Ruan, S. Maisonneuve

and J. Xie, *Dyes and Pigments*, 2011, **90**, 290-296; (i) H. Sakamoto, J. Ishikawa, S.

Nakao and H. Wada, *Chem. Commun.*, 2000, **23**, 2395-2396.

20 L. M. Hu, Z. Y. Chen, S. M. Lu, X. S. Li, Z. J. Liu, H. S. Xu. *Phosphorus, Sulfur and Silicon and the Related Elements*, 2004, **179**, 1065-1073.

21 P. Venkatesan, S. P. Wu. *Analyst*, 2015, **140**, 1349-1355.

22 G. A. Crosby, J. N. Demas. *J. Phys. Chem.*, 1971, **75**, 991-1024.

Figure captions:

**Scheme 1** Synthetic route to compound **1**.

**Fig.1** (A) Fluorescence spectra of compound **1** (10  $\mu\text{M}$ ) in acetonitrile-water solution (1:1  $V/V$ , 50 mM PBS buffer solution at pH 7.4) at various concentrations of  $\text{ClO}^-$  (0-130  $\mu\text{M}$ ); (B) the right figure displays the fluorescent intensity vs the  $\text{ClO}^-$  concentration.

**Fig.2** UV-vis spectra of 30  $\mu\text{M}$  compound **1** in the absence of  $\text{ClO}^-$  (red line) and in the presence of  $\text{ClO}^-$  (black line). Inset: the photographic images of compound **1** in the presence of and in the absence  $\text{ClO}^-$  under ultraviolet lamp irradiation.

**Fig.3** Time-dependent fluorescence intensity changes of compound **1** (10  $\mu\text{M}$ ) in the absence (a), in the presence of 50  $\mu\text{M}$  (b) and the presence of 120  $\mu\text{M}$   $\text{ClO}^-$  (c) in acetonitrile-water solution (1:1  $V/V$ , 50 mM PBS buffer solution at pH 7.4).

**Fig.4** Fluorescence intensities of 10  $\mu\text{M}$  compound **1** in the absence (a) and the presence of 120  $\mu\text{M}$  (b) in acetonitrile-water solution (1:1  $V/V$ , 50 mM PBS buffer) at various pH with 120  $\mu\text{M}$   $\text{ClO}^-$ .

**Fig.5** Fluorescence emission spectra of 10  $\mu\text{M}$  compound **1** in the absence (a) and the presence of 120  $\mu\text{M}$  (b) in acetonitrile-water solution (1:1  $v/v$ , 50 mM PBS buffer solution at pH 7.4) with various analyte (120  $\mu\text{M}$ ).

**Scheme 2** Proposed mechanism for the response of compound **1** to  $\text{ClO}^-$ .

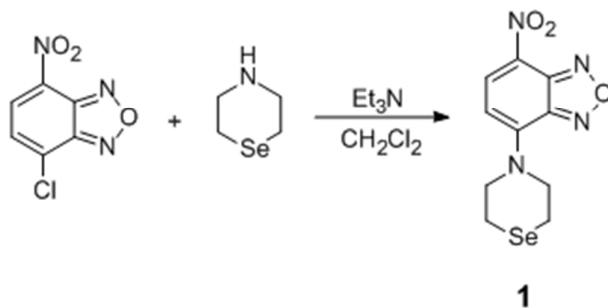
**Fig.6** Fluorescence response monitored at 544 nm after each addition. (a), (c), (e), (g): after addition of 12 eqv.  $\text{ClO}^-$ . (b), (d), (f), (h): after addition of GSH.

**Fig.7** Job's plot diagram of compound **1** for  $\text{ClO}^-$ .

**Fig.8** Fluorescence microscopy images of Hela cells. (A) Images of cells pre-treated

with compound **1** (10  $\mu\text{M}$ ) for 30 min at 37°C. (C) Images of cells incubated subsequent with NaClO (30  $\mu\text{M}$ ) solution for 30 min at 37°C. (E) Images of cells further incubated with compound **1** with GSH (100  $\mu\text{M}$ ) for 30 min at 37°C. (B), (D) and (F) represent the bright-field images of (A), (C) and (E) respectively.

**Table 1** A comparison of various approaches to ClO<sup>-</sup> detection.



Scheme 1 Synthetic route to compound 1

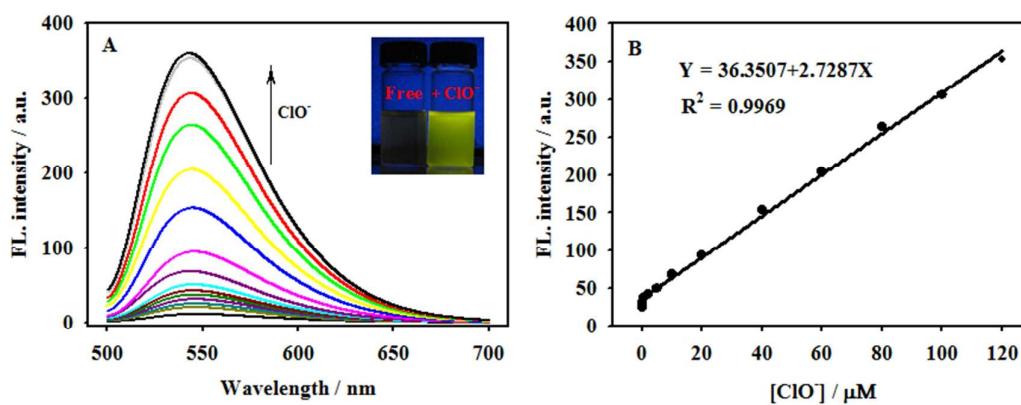


**Fig.1** (A) Fluorescence spectra of compound **1** ( $10\ \mu\text{M}$ ) in acetonitrile-water solution (1:1  $V/V$ , 50 mM PBS buffer solution at pH 7.4) at various concentrations of  $\text{ClO}^-$  (0-130  $\mu\text{M}$ ); (B) the right figure displays the fluorescent intensity vs the  $\text{ClO}^-$  concentration.

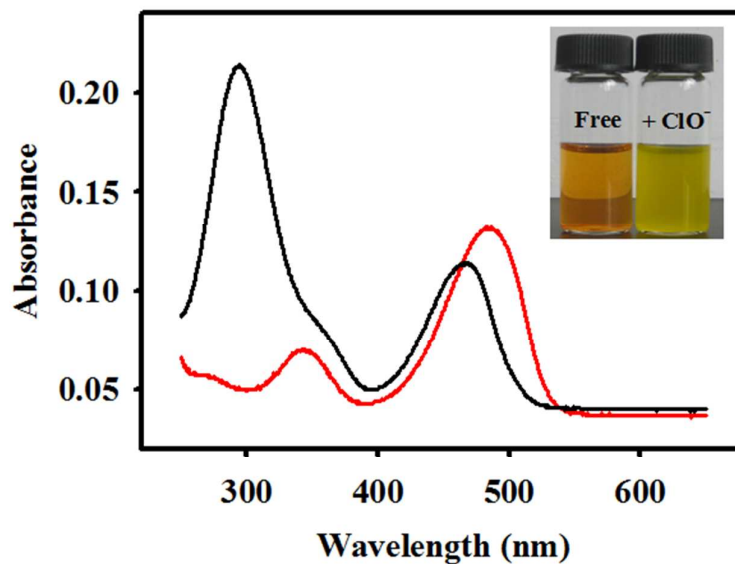


**Fig.2** UV-vis spectra of 30  $\mu\text{M}$  compound **1** in the absence of  $\text{ClO}^-$  (red line) and in the presence of  $\text{ClO}^-$  (black line). Inset: the photographic images of compound **1** in the presence of and in the absence  $\text{ClO}^-$  under ultraviolet lamp irradiation.

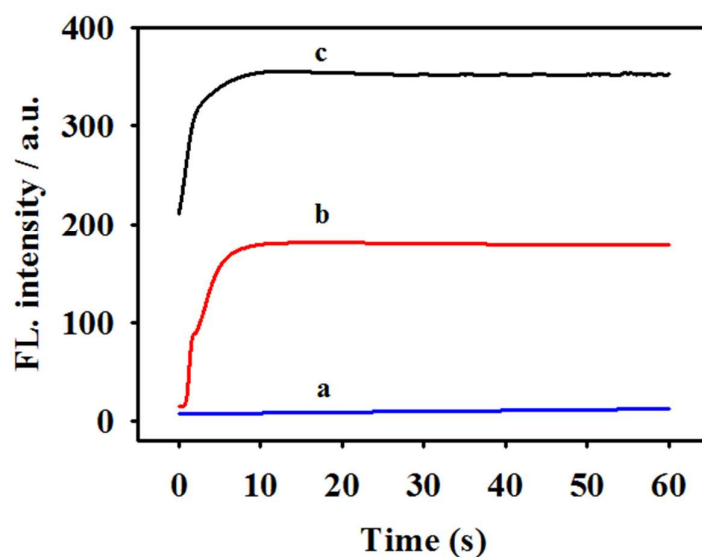


**Fig. 3** Time-dependent fluorescence intensity changes of compound **1** (10  $\mu\text{M}$ ) in the absence  $\text{ClO}^-$  (a), in the presence of 50  $\mu\text{M}$   $\text{ClO}^-$  (b) and in the presence of 120  $\mu\text{M}$   $\text{ClO}^-$  (c) in acetonitrile-water solution (1:1  $V/V$ , 50 mM PBS buffer solution at pH 7.4).

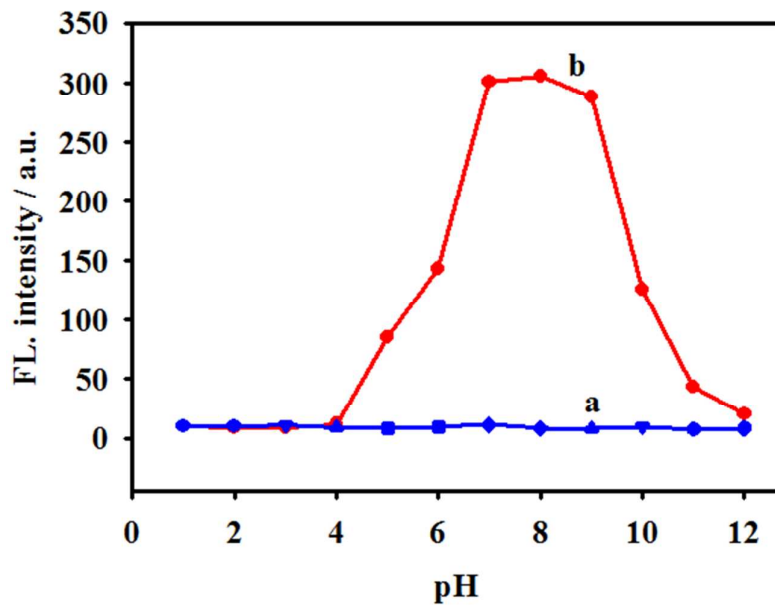


**Fig.4** Fluorescence intensities of 10  $\mu\text{M}$  compound **1** in the absence (a) and the presence of 120  $\mu\text{M}$  (b) in acetonitrile-water solution (1:1  $V/V$ , 50 mM PBS buffer ) at various pH with 120  $\mu\text{M}$   $\text{ClO}^-$ .

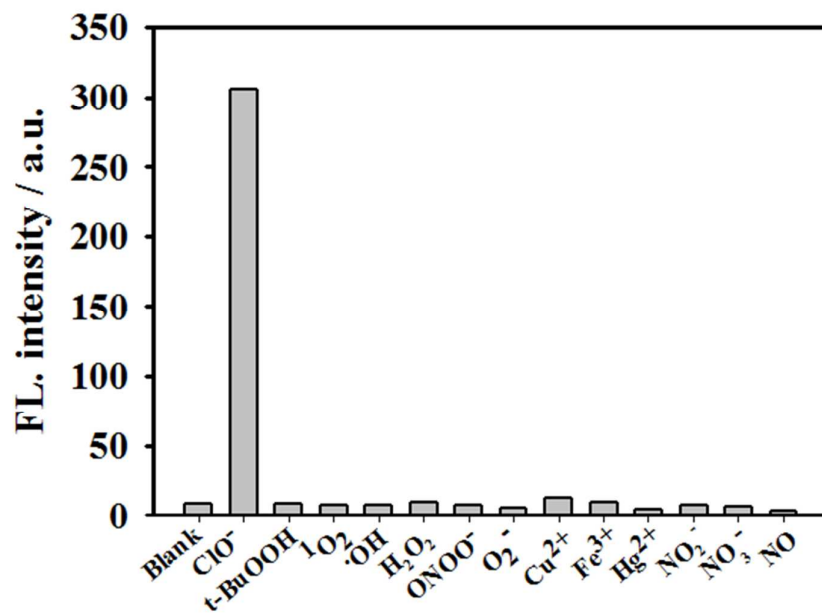


**Fig. 5** Fluorescence emission spectra of 10  $\mu\text{M}$  compound **1** in acetonitrile-water solution (1:1 v/v, 50 mM PBS buffer solution at pH 7.4) with various analyte (120  $\mu\text{M}$ ).

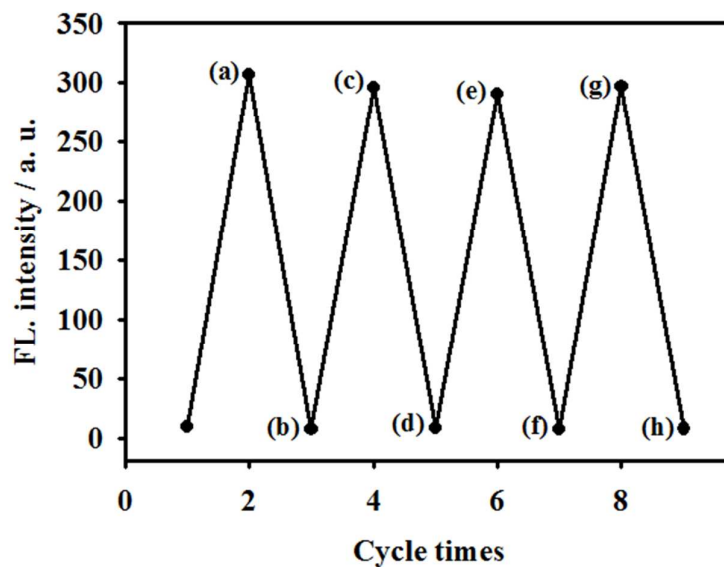
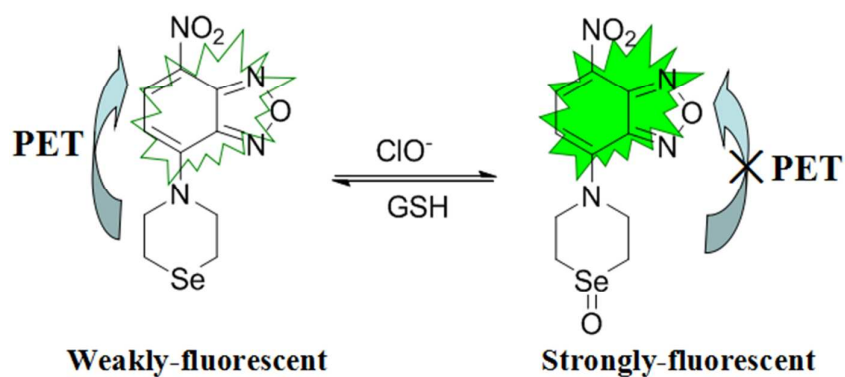


**Fig.6** Fluorescence response monitored at 544 nm after each addition. (a), (c), (e), (g): after addition of 12 eqv.  $\text{ClO}^-$ . (b), (d), (f), (h): after addition of GSH.



**Scheme 2** Proposed mechanism for the response of compound **1** to  $\text{ClO}^-$

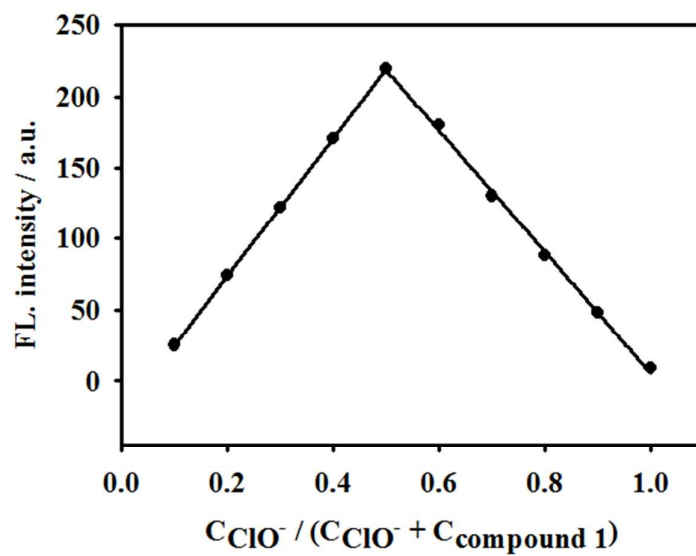


**Fig.7** Job's plot diagram of compound **1** for ClO<sup>-</sup>.

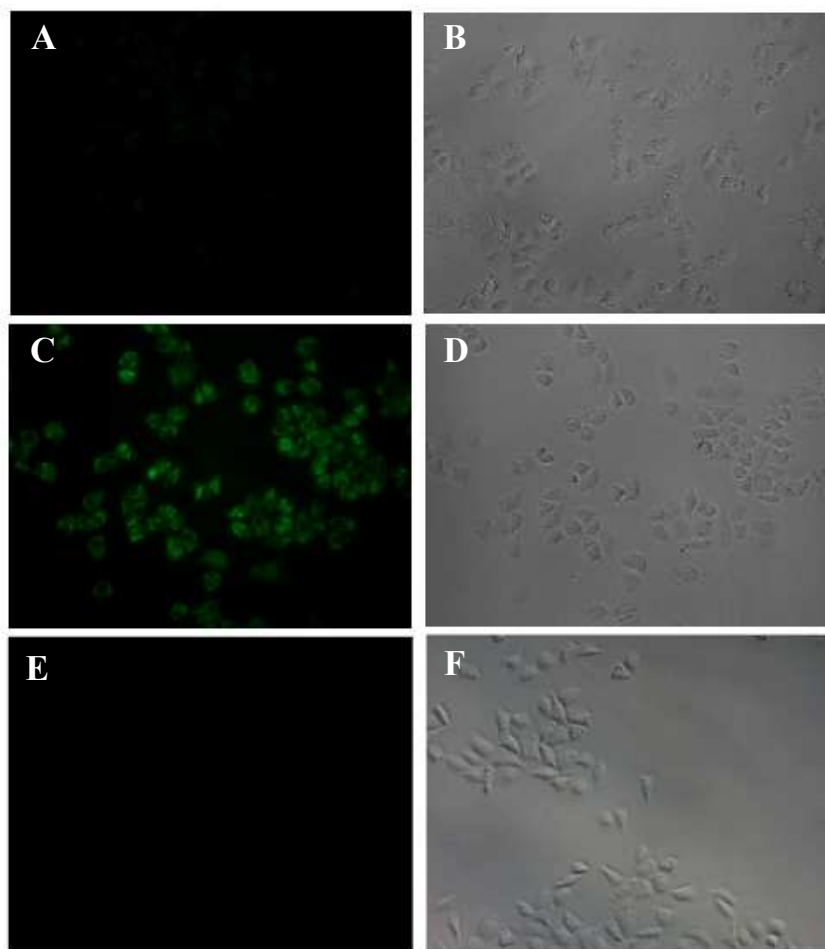


**Fig.8** Fluorescence microscopy images of HeLa cells. (A) Images of cells pre-treated with compound **1** ( $10\ \mu\text{M}$ ) for 30 min at  $37^\circ\text{C}$ . (C) Images of cells incubated subsequent with  $\text{NaClO}$  ( $30\ \mu\text{M}$ ) solution for 30 min at  $37^\circ\text{C}$ . (E) Images of cells further incubated with compound **1** with GSH ( $100\ \mu\text{M}$ ) for 30 min at  $37^\circ\text{C}$ . (B), (D) and (F) represent the bright-field images of (A), (C) and (E) respectively.

**Table 1** A comparison of various approaches to ClO<sup>-</sup> detection

Detection method	Detection limit (M)	Testing media	Reaction time	Linearly range (μM)	Ref.
Irreversible fluorometry	$1.98 \times 10^{-8}$	DMF / Phosphate buffer (20 mM, pH 7.4; 0.5:100, v/v)	6 min	0-20	12a
Irreversible fluorometry	$4.48 \times 10^{-9}$	HEPES buffer (20 mM, pH 7.4)	30 min	0.5-5	12m
Irreversible fluorometry	$10 \times 10^{-9}$	PBS buffer (10 mM, pH 7.4)	30 min	0-6.4	12p
Reversible fluorometry	$41.3 \times 10^{-9}$	CH <sub>2</sub> OH / PBS (100 mM, pH 7.4; 1:99, v/v)	200 s	0-10	21
Reversible fluorometry	$5.86 \times 10^{-7}$	PBS buffer (20 mM, pH 7.40)	15 min	0-15	15d
Reversible fluorometry	$9.8 \times 10^{-7}$	CH <sub>3</sub> CN / PBS (20 mM, pH 7.4; 3:7, v/v)	5 min	0-70	15c
Reversible fluorometry	$3.3 \times 10^{-9}$	CH <sub>3</sub> CN / PBS (50 mM, pH 7.4; 1:1, v/v)	10 s	0.05-120	This work